CHARACTERIZATION OF Ni/ Ag THIN FILMS

PhD DISSERTATION

MYO MON MON WYNN

DEPARTMENT OF PHYSICS
UNIVERSITY OF YANGON
MYANMAR

MAY 2011

ABSTRACT

Thin films of silver sulfide (Ag_2S) have been chemically deposited from an alkaline bath, using sodium thiosulphate as a sulphur source, onto glass and metal substrates (Ni) by a simple and economical electroless chemical deposition technique. Their structural, optical and electrical properties have been studied. X- ray studies of the films showed that the as-prepared films of Ag_2S were a mixture of both amorphous and polycrystalline phases, while Ag_2S/ Ni films were found to be polycrystalline. Annealing of the films of Ag_2S and Ag_2S/ Ni at 200 ºC for 3 h led to further crystallization. The films contained a random distribution of small crystallites and at annealing temperature 200°C show the over-growth of particles on the smooth film surface. The optical band gap of the Ag_2S thin films was evaluated from the analysis of the absorption spectra and estimated to be between 2.2 eV- 2.4 eV. Rise and decay of photoconductivity was studied at room temperature. The sheet resistance was 10^6 Ω/ square and electrical resistivity is of the order of 10^2-10^3 Ω cm, determined by Van der Pauw four- point probe method. Sheet carrier density, hall mobility can be determined from Hall Effect measurement. Variation of magnetoresistance and Hall voltage measurement was determined.

ACKNOWLEDGEMENTS

I would like to express my particular thanks to Professor Dr Win Win Thar, PhD, Head of Department of Physics, University of Yangon for her kind permission to undertake this research.

I am greatly indebted to Supervisor Dr Pho Kaung, DSc(*Hokkaido*), MInstP(*London*), Pro-Rector & Director, Universities' Research Centre, University of Yangon for his guidance.

LIST OF FIGURES

LIST OF TABLES

CONTENTS

CHAPTER I

INTRODUCTION

The semiconductive metal chalcogenides represent an interesting class of materials which are attractive for large- scale applications because of the easy availability and low cost of the starting materials. The utilization of these promising semiconductive materials needs low cost production and pollution-free technique. The deposition of materials in the thin film form has been the subject of intense research over the past decades due to applications in various fields such as antireflection coatings and optical filters, surface acoustic wave devices, electronic components (both discrete and integrated), fabrication of large area photodiode arrays, solar selective coatings, solar cells, photoconductors, sensors, etc. The chemical deposition methods are low cost processes and the films are found to be of comparable quality to those obtained by more sophisticated and expensive physical deposition process.

Among these chemical methods, chemical bath deposition (CBD) which is also known as solution growth, controlled precipitation, or simply chemical deposition, recently has emerged as the method for the deposition of metal chalcogenide thin films [5]. The CBD method is presently attracting considerable attention, as these do not require sophisticated instrumentation like vacuum system and other expensive equipments. Simple equipments like hot plate with magnetic stirrer are needed. The starting chemicals are commonly available and cheap. Thiourea, thioacetamide, thiosulphate and sodium sulfide are generally used as sulfide precursors. Metallic precursors are metal complexed ions with ammonia ligands, for instance [2].

In addition, a drastic cut in the cost of production of semiconductor devices is possible by the use of semiconducting thin films in place of single crystals.

Most of the semiconducting metal chalcogenides are important materials for applications in various photoelectric and other kinds of devices. Thin films of metal chalcogenides can be deposited on glass, metal, plastics and other substrates by a variety of techniques, such as pyrolysis, sputtering, evaporation and chemical deposition. The optical and electrical characteristics of the deposited materials often depend on the deposition technique used.

Various techniques are available for the preparation of chalcogenide thin films. It is well known that silver sulfide has been used in various optical and electronic devices, such as photoconducting cells, IR detectors, solar selective coatings and photovoltaic cells. The chemical deposition process is at present attracting considerable attention, since it offers the advantages of economy, convenience and the capacity for large area deposition of II-VI, V-VI, I-III-VI, etc. compound thin films [1,7]. These films are formed by reaction between complex metal ions and sulfide (HS- or S^{2-}) ions. The latter are formed slowly by hydrolysis of thiourea, thioacetamide and sodium thiosulphate ($Na_2S_20_3$) on a variety of substrates, such as insulators, metals and semiconductors. Stoichiometric deposits are easily obtained since the basic building blocks are ions in chemical bath deposition. The film forms slowly; this facilitates better orientation of crystallites with improved grain structures, depending on deposition conditions such as the bath temperature, stirring rate, pH, solution concentration, solution purity, and substrate quality. Film growth can take place by ion-by-ion condensation of the material on the substrate. Chemical deposition of thin films of Ag_2S from an alkaline medium has been reported by Mangalam *et al.* [6] and Dhumure and Lokhande [3, 4]. It is observed that the films are uniform, thick, adherent and photoconductive. The optical band gap was estimated to be 0.80 eV. The X-ray diffraction (XRD) pattern indicated that the films are microcrystalline. Recently, Dhumure and Lokhande [4] have reported on chemical deposition of thin films of Ag_2S from an acidic medium using thioacetamide as a sulfide ion source. It was observed that the films were thin and adherent to the substrates, polycrystalline and n-type in conductivity.

In this work, a chemical method for the deposition of Ag_2S films from an alkaline medium using $Na_2S_20_3$ as a sulfide ion source is reported. The structural, optical and electrical properties of the films were studied. The optimal chemical bath composition for each kind of film is specified, as well as other relevant conditions for obtaining uniform, mirror- like thin films.

CHAPTER II

MATERIALS AND METHODS

Thin films of Ag_2S have been chemically deposited from aqueous alkaline bath using sodium thiosulphate as a sulphur source, onto glass as well as metal substrates. Their structural, optical and electrical properties have been studied. The most widespread use of X-ray powder diffraction is for the identification of crystalline compounds by their diffraction patterns of as- prepared and annealed Ag_2S thin films on glass substrate and metal (Ni) substrate. Morphology and microstructure properties of the as- deposited and annealed films on different substrates were studied using a Scanning Electron Microscopy (SEM). Optical absorption/ transmission spectra were carried out using Shimadzu (UV-240) UV/ VIS double beam spectrophotometer. Sheet resistance and electrical resistivity values of all films were determined by four-point probe method. Hall Effect measurement is a unique tool to provide basic material parameters needed to find the suitability of its application.

2.1. Basics of Chemical Bath Deposition

Most of the chemical baths (medium) consists of one or more metal salts M^{n+}, a source for the chalcogenide X (X= S, Se, Te), and typically a complexing agent, in an aqueous solution. The deposition of metal chalcogenide occurs via following four steps.

(1) Equilibrium between the complexing agent and water;

(2) Formation/dissociation of ionic metaleligand complexes $[M\ (L)_i]^{n-ik}$, where L^{k-} denotes one or more ligands;

(3) Hydrolysis of the chalcogenide source; and

(4) Formation of the solid.

During the step 3, the metal cations are pulled out of solution by the desired non-metal species provided through the hydrolysis of the chalcogenide source, to form the solidfilm. The kinetics of the step 3 is highly sensitive to the solution pH and temperature, as well as to the catalytic effects of certain solid species that may be present, which in turn decides rates of the formation of thin film on the surface of the substrate or bulk precipitation. The basic principle involved behind the formation of desired solid film/bulk M_mX_n (step 4) is the rising concentration of X^{m-} from step 3 causes the ionic product $[M^{n+}]^m [X^{m-}]^n$ to exceed the solubility product. During step 2, the formation of complexed metal ions allows control over the rate of formation of solid metal hydroxides, which competes with step 4 and which would otherwise occur immediately in the normal alkaline solutions. These steps together determine the composition, growth rate, microstructure, and topographies of the resulting thin films. The oxide deposition using CBD method also takes place by following above four reaction steps. Step 1 in those cases where a complexing agent is used, in the same for the non-oxide and oxide depositions, where the function of the ligand remains one of slowing down the rate of solid formation. The analogous process to step 3, hydrolysis of the chalcogenide source, is essentially the dissociation reaction of water.

$$nH_2O \leftrightarrow nOH^- + nH^+ \qquad (1)$$

Step 2, the association/dissociation equilibrium of the solvated metal complex, can be thought of as being replaced by a process in which the ligands of the complex are displaced by hydroxyl groups to form a solid hydroxide compound.

$$nOH^- + M(L)_i^{(n-ik)+} \rightarrow M(OH)_n(S) + iL^{k-} \qquad (2)$$

where, M^{n+} is a metal cation complexed by i ligands L^{k-}. The formation of oxide can come about via deprotonation of the hydroxide compound to form the oxide (step 4).

$$M(OH)_n(S) \rightarrow MO_{n/2}(S) + (n/2)H_2O \quad (3)$$

However, the processes depicted from reactions (2) and (3) are sometimes called as a forced hydrolysis. In most of the reported literature, the hydroxide was converted to the oxide only after heating the as-deposited film at 423-673 K. Therefore, the net general oxide formation scheme can be written as;

$$M(L)_i^{(n-ik)+} + (n/2)H_2O \rightarrow MO_{n/2}(S) + nH^+ + iL^{k-} \quad (4)$$

2.2 Simple Ion-by-Ion Mechanism

In most of the CBD's, the 'ion-by-ion' conceptually simplest mechanism, often assumed to be the operative one in general. It occurs by sequential ionic reactions. The general reaction for the mechanism

$$M^{n+} + X^{m-} \rightarrow M_mX_n \text{ (Adsorbed on the substrate)} \quad (5)$$

The formation of solid M_mX_n is based on the principle that when the ion product, $[M^{n+}][X^{m-}]$, exceeds the solubility product, K_{sp}, of M_mX_n, thenM_mX_n can form as a solid phase, although a larger ionic product may be required if supersaturation occurs. If the ion product does not exceed K_{sp}, no solid phase will form, except possibly transiently due to local fluctuations in the solution, and the small solid nuclei will redissolve before growing to a stable size. For

that reason, the precipitation process is an equilibrium rather than as a one-way reaction.

2.3 Film Formation Mechanism

The mechanism of Ag_2 S film formation can be assumed to proceed as follows:

(1) Formation of a complex with silver,

$AgNO_3 + NH_3 \rightarrow Ag(NH_3)NO_3$;

(2) Diffusion of $Ag(NH_3)NO_3$, OH^- and thickness of the catalytic surface of Ag_2S,

(3) $H_2N—\overset{\overset{\|}{S}}{C}—NH_2 + OH \rightarrow CH_2N_2 + H_2O + HS$;

(4) $HS^- + OH^- \rightarrow S^{2-} + H_2O$;

(5) $2[Ag(NH3)]^+ + S^{2-} \rightarrow Ag_2S + 2\ NH_3$

2.4 Experimental Setup of Chemical Bath Deposition

The chemical bath deposition (CBD) experimental setup is shown in Fig. 2.1. In this method, substrates are stationary and solution is stirred with the help of magnetic stirrer. Glass of up to 100 ml total volume has been used to insert substrates the size of a standard microscope glass slide (7.5 cm× 2.5 cm× 0.1 cm). Water or paraffin baths with constant stirring are used to heat the chemical bath to the desired temperature. In some cases, stirring is continuous from room temperature, while in some cases, it is started after attaining the desired temperature.

CHAPTER III

STRUCTURAL PROPERTIES OF CHEMICALLY DEPOSITED Ag_2S THIN FILMS

Thin, uniform and adherent Ag_2S films have been chemically deposited from aqueous alkaline bath was undertaken. Thin films of Ag_2S were deposited by a simple electroless technique on glass and metal (Ni) substrates, as prepared and annealed films at 200 °C for 3 h. The deposition films of as prepared Ag_2S films on glass substrate were found to be a mixture of both amorphous and polycrystalline phases, while annealed films were polycrystalline. Both as-prepared and annealed Ag_2S/ Ni films were polycrystalline phases. The lattice parameters, average crystallite size were observed. The surface morphology of the films of 0.09μm thickness, deposited in about 1 h from multiple dips from fresh chemical bath was studied and the grain size can be estimated from different micrographs.

3.1 Film Thickness Measurement

Thickness of the film is an important parameter to be measured because most of film properties are thickness dependent. Thickness of the films was estimated by the weight difference method. The microbalance was used to find out the weight of the Ag_2S films and by assuming the density of the film as that of the bulk Ag_2S ($7.23 gcm^{-3}$), weighing- method was employed for film thickness measurement using the following relation:

$$t = \frac{\Delta m}{\rho A}$$

where, ρ is the bulk density of material of film deposited on area A and Δm the mass of the film deposited. The films of thickness up to 0.09 μm were obtained by re- introducing the initially deposited films into a fresh bath.

3.2 X ray Diffraction Analysis of Ag_2S Thin Films on Glass Substrate

In the present investigation, the XRD patterns of as prepared (as prep.) and annealed Ag_2 S films on glass substrates are shown in Fig 3.1 and 3.2, respectively. It was observed that the as- prepared films were a mixture of both amorphous and polycrystalline phases. From some broad peaks observed in the XRD pattern of the "as prepared film", it is concluded that they pertain to the monoclinic phase, as expected from the temperature employed in chemical bath deposition. Annealing of the films at 200 ºC for 3 h led to further crystallization and a polycrystalline phase was obtained. The d values were determined by using the relation for a monoclinic crystal system.

$$\frac{1}{d2} = \frac{1}{\sin 2\beta}\left(\frac{h2}{a2} + \frac{k2\sin 2\beta}{b2} + \frac{l2}{c2} - \frac{2hl\cos\beta}{ac}\right)$$

Where, β=99.34°, a=4.2467 Å, b=6.8424 Å and c=7.8951 Å. In the case of the films annealed at 200 ºC, there is an increased in the intensity of the peaks due to reflections from (012) planes (2θ= 26.323º) and (-112) planes (2θ= 31.444º), and (111) planes (28.869º) of the acanthite phase.

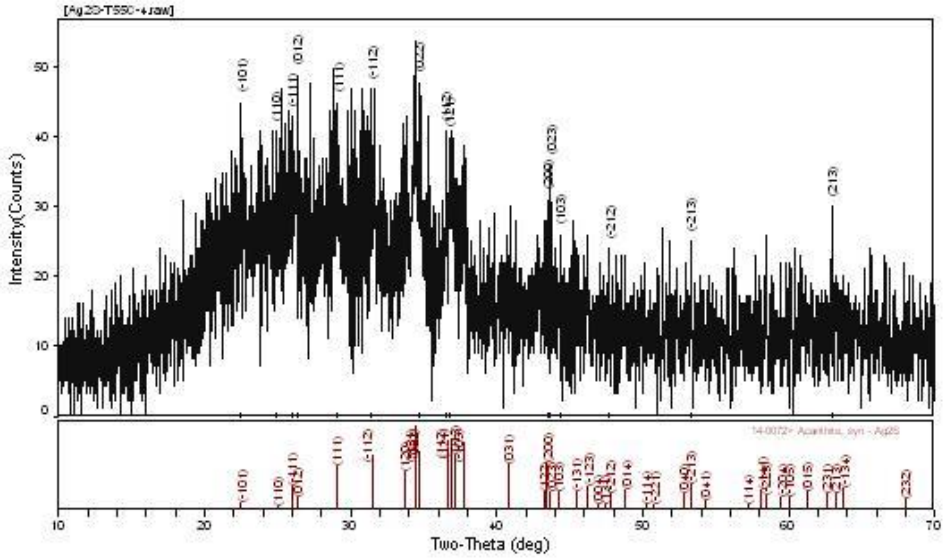

Fig 3.1 XRD pattern recorded for as prepared Ag_2S thin films on glass substrate

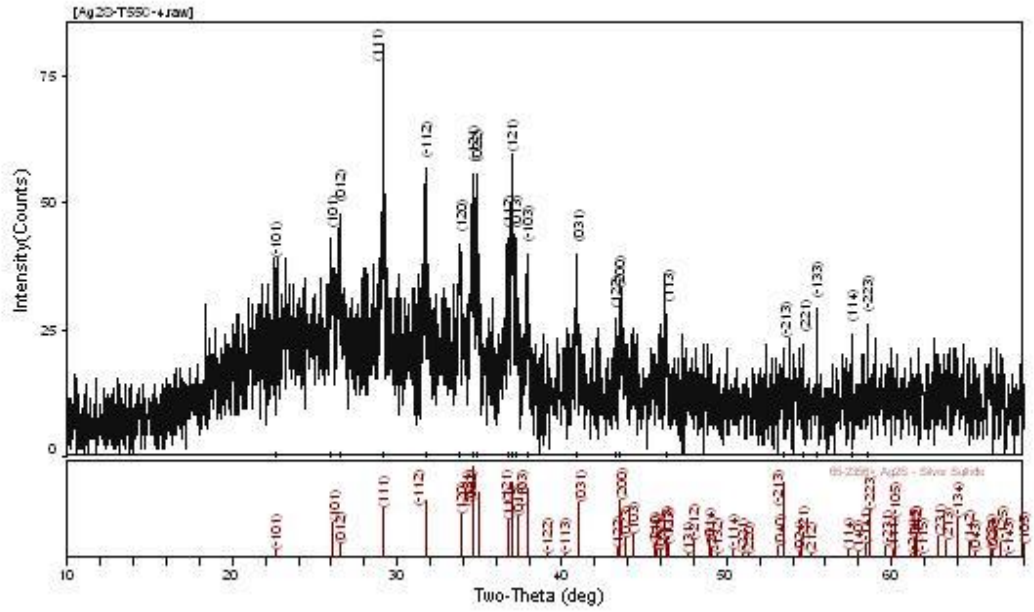

Fig 3.2 XRD pattern of Ag_2S thin films on glass substrate after annealing in air at 200ºC for 3 h

Table 3.1 Comparison of d- values, FWHM and crystallite size of Ag_2S films thickness, 0.09 µm on glass substrate

Film	Standard *d*- values (Å)	Observed *d*- values (Å)	Reflection plane (hkl)	FWHM (rad)	Crystallite Size (nm)
Ag_2S (as prepared)	3.0800	3.0901	(111)	7.557×10^{-3}	18.95
Ag_2S (annealed)	3.0649	3.0602	(111)	$2.112\text{x}10^{-3}$	68.06

Table 3.2 Comparison of d- values, FWHM and crystallite size of as prepared Ag_2S/ Ni films thickness, 0.09 µm

Film	Standard *d*- values (Å)	Observed *d*- values (Å)	Reflection plane (hkl)	FWHM (rad)	Crystallite Size (nm)
Ag_2S/ Ni (as prepared)	2.0809	2.0805	(200)	3.106×10^{-3}	48.05
Ag_2S/ Ni (annealed)	2.0707	2.0759	(023)	2.635×10^{-3}	56.92

3.3 X ray Diffraction Analysis of Ag_2S Thin Films on Ni Substrate

Metal substrate (Ni) was successfully used with this technique, to deposit thin films up to 0.09 μm thick from multiple dips in fresh baths. The crystalline structure evidenced for the as- deposited and annealed films matches well that of the monoclinic acanthite phase of Ag_2S. X- ray diffraction patterns recorded for as prepared and annealed Ag_2S/ Ni were observed in Fig 3.3 and 3.4, respectively.

Thus, it is established that the films deposited on glass substrates and nickel (Ni) substrates reported here conform to the monoclinic phase, the crystalline nature of which improves upon heating in air at 200 ºC. The observed lattice parameters can be obtained by indexing the first five reflections for Ag_2S/ Ni are: a= 4.2166 Å, b= 6.8364 Å and c= 7.9044 Å and β= 99.73º. Comparison of d- values, FWHM and crystallite size of as prepared Ag_2S/ Ni films thickness, 0.09 μm was presented in Table 3.3.

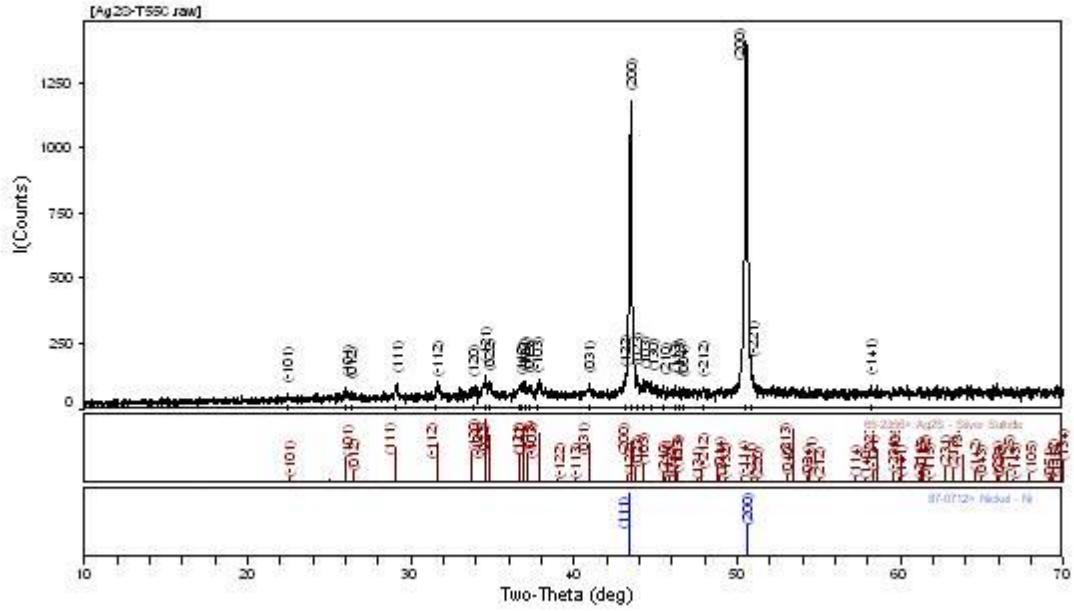

Fig 3.3 XRD pattern of as prepared Ag_2S/ Ni thin films

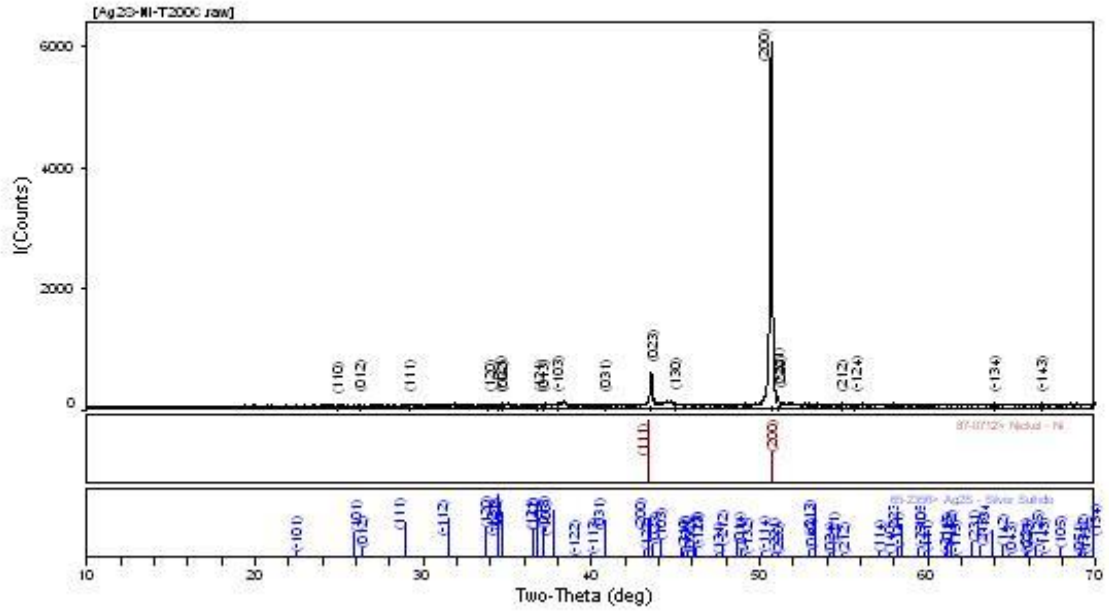

Fig 3.4 XRD pattern recorded for annealed Ag_2S/ Ni thin films in air at 200ºC for 3 h

3.4 Determination of Crystallite Size

The crystallite size (D) of the films for the peak with highest intensity can be estimated by using Scherrer's formula ,

$$D = \frac{0.9\lambda}{\beta \cos\theta}$$

where, λ is the X-ray wavelength used, β is the full width at half maximum of the diffraction peak in radian, and θ is Bragg's diffraction angle. It is observed that XRD pattern of as prepared Ag_2S on glass substrate shows a preferred orientation along (111) plane and a monoclinic phase with 43.28 nm average crystallite size. The presence of sharp structural peaks in these X- ray diffraction patterns confirmed the polycrystalline nature of the films. As shown in Fig 3.3, as prepared Ag_2S/ Ni film has (200) as the preferred orientation with 49.32 nm average crystallite size.

3.5 Morphology of Ag_2S Thin Films

In chemical bath deposition of semiconductor thin films, it is known that the entire process passes through a nucleation phase, growth phase and a terminal phase [2]. The morphology of the film surface is subject to change during the deposition process, because there are competing processes of ion-by-ion deposition and incorporation of clusters formed in the bulk of the bath into the film. This is known to give rise to distinct types of quantum confinement of the charge carriers as well [8].

In the case of chemically deposited Ag_2S thin films reported here, roughness of the surface has been observed towards the terminal phase. At this stage of the deposition, the film thickness does not increase, but the roughness increases— the film surface loses its specularly reflective nature due to optical scattering from the particulates. The surface morphology of the as prepared and annealed films of thickness 0.09 μm Ag_2S and Ag_2S/ Ni was shown in Fig 3.5 and 3.6, respectively.

After annealing in air at 200 ◦C for 3h, both films become smoother. The calculated average grain size of as prepared and annealed Ag_2S films found to be 0.83 μm and 0.57 μm, respectively. And the values of average grain size of as deposited and annealed Ag_2S/ Ni at 200 °C were 0.64 μm each.

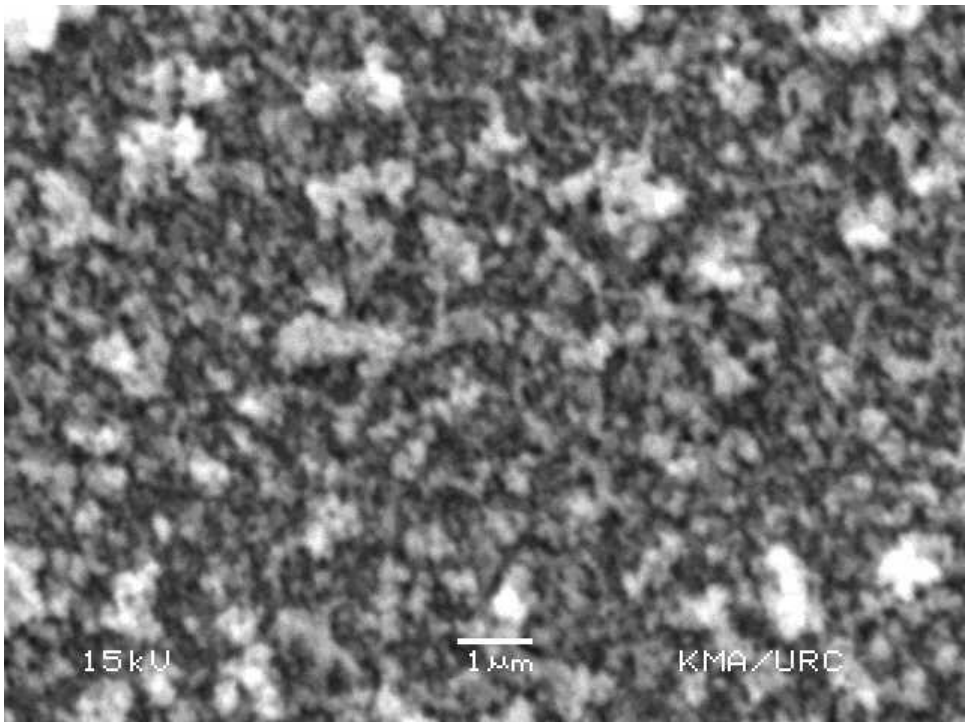

(a)

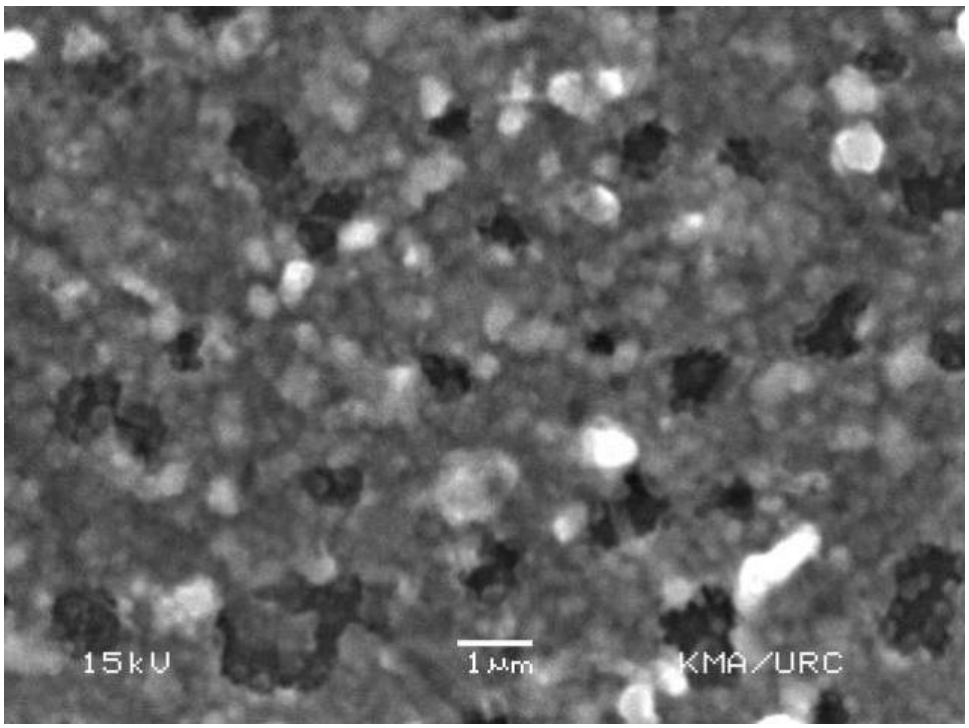

(b)

Fig 3.5 SEM images of (a) as- deposited and (b) annealed films of Ag_2S

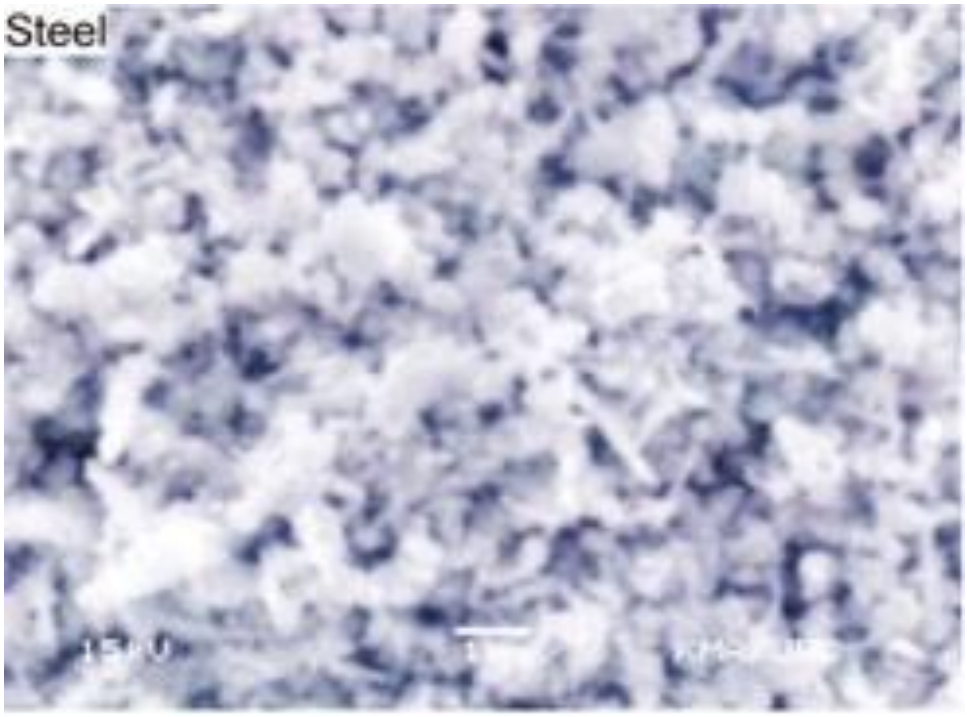

(a)

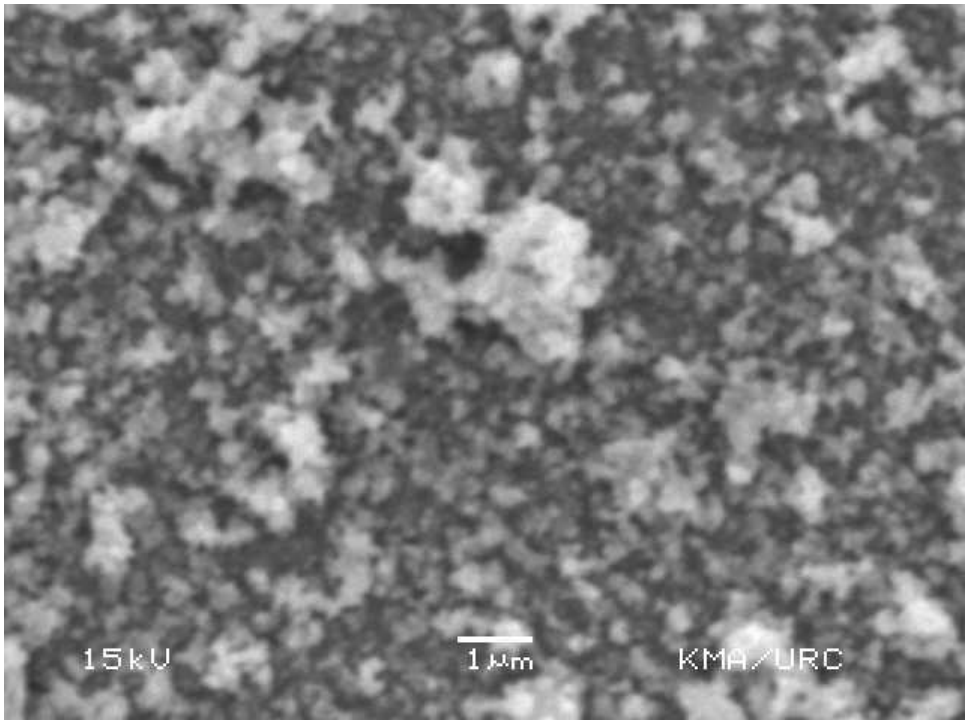

(b)

Fig 3.6 SEM images of (a) as- deposited and (b) annealed films of Ag_2S/ Ni

CHAPTER IV

OPTICAL PROPERTIES OF Ag_2S THIN FILMS

Optical absorbance/ transmittance measurements of Ag_2S films were carried out using Shimadzu UV/ VIS double beam spectrophotometer in the wavelength range of 300 nm- 700 nm. The film properties investigated include their absorbance, transmittance spectra, band gap, refractive index, extinction coefficient, optical conductivity were made for calculation of optical properties. Films deposited at 55ºC showed a sharp decrease in αt with increasing wavelength λ. As prepared films for different deposition cycles have a direct optical band gap of varied from 2.2- 2.4 eV.

4.1 Basic principles of Spectrophotometry

Spectrophotometer is an instrument that measures the fraction of the incident light transmitted through a solution. In other words, it is used to measure the amount of light that passes through a sample material and, by comparison to the initial intensity of light reaching the sample, they indirectly measure the amount of light absorbed by that sample. Spectrophotometers are designed to transmit light of narrow wavelength ranges shown in Fig 4.1.

A given compound will not absorb all wavelengths equally–that's why things are different colors (some compounds absorb only wavelengths outside of the visible light spectrum). Because different compounds absorb light at different wavelengths, a spectrophotometer can be used to distinguish compounds by analyzing the pattern of wavelengths absorbed by a given sample. Additionally, the amount of light absorbed is directly proportional to the concentration of absorbing compounds in that sample, so a spectrophotometer can also be used to determine concentrations of compounds in solution. Finally, particles in suspension will scatter light (thus preventing it from reaching the light

detector), spectrophotometers may also be used to estimate the number of cells in suspension. We will be using a spectrophotometer several times this semester to quantify the concentration of chemicals present in a solution.

Visible light (400-700 nm) constitutes only a small portion of the spectrum that ranges from gamma rays (less than 1 pm long) to radio waves that are thousands of meters long. When studying a sample by spectrophotometry, we put it in a sample holder called a cuvette and place it in the spectrophotometer. Light of a particular wavelength passes through the sample inside the cuvette and the amount of light transmitted (passed through the solution—Transmittance) or absorbed (Absorbance) by the sample is measured by a light meter.

A spectrophotometer can display measurements as either transmittance or absorbance. The amount of light transmitted through a sample is referred to as transmittance (T). The transmittance is defined as the ratio of the light energy transmitted through the sample (I) to the energy transmitted through the reference blank (I_0). Since the compound being tested is not present in the reference blank, the transmittance of the reference blank is defined as 100%T.

$$T = \frac{I}{I_0}$$

Absorbance is related logarithmically to transmission thusly.

$$A = -\log T$$

The light from the spectrophotometer's light source (in the case of measurements in the visible range, a simple incandescent bulb) does not consist of a single wavelength, but a continuous portion of the electromagnetic spectrum. This light is separated into specific portions of the spectrum through

the use of prisms or a diffraction grating. A small portion of the separated spectrum then passes through a narrow slit.

When you adjust the wavelength on a spectrophotometer, we are changing the position of the prism or diffraction grating so that different wavelengths of light are directed at the slit. The smaller the slit width, the better the ability of the instrument to resolve various compounds. The slit width is < 8 nm. Very high quality spectrophotometers have slit widths of < 2 nm. This small band of light then passes through the cuvette containing the sample. Light that passes through the sample is detected by a photocell and measured to yield the transmittance or absorbance value (optical density) for the sample.

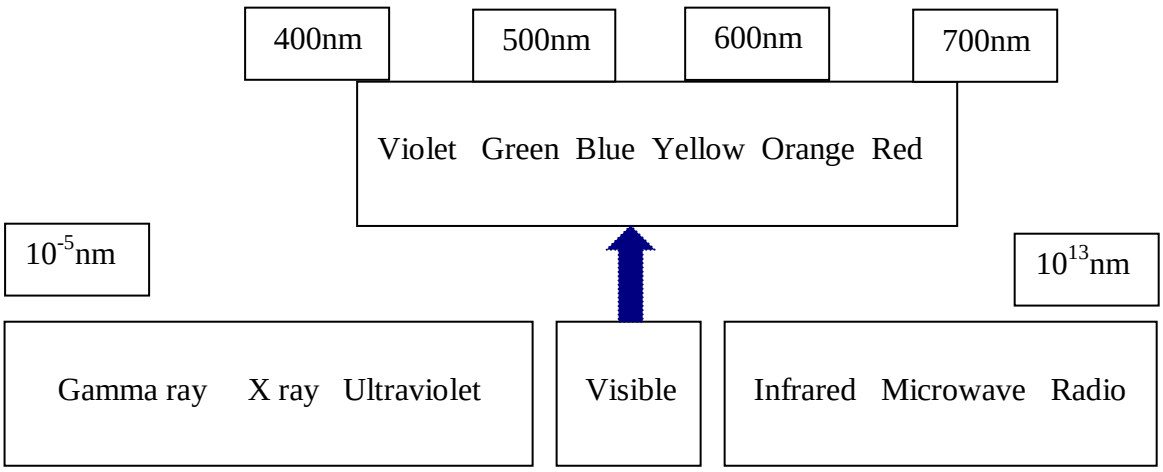

Fig 4.1 The electromagnetic spectrum

4.2 The Energy Band Model

Direct Gap Semiconductors: Fig 4.2(a) shows the **E** versus **k** plots for direct gap semiconductor along the [100] and [111] directions. It is seen that the lowest conduction band minimum and the valence band maximum are saturated at the same values of **k**. The semiconductors with this type of structure are called direct gap semiconductors. The significance of this term is that a photon of energy $E_g = h\nu$ can excite an electron from the top of the valence band directly into a state at the bottom of the conduction band [9]. If the photon energy $h\nu > E_g$, the excess energy is shared between the electron and the hole, and both have the same value of **k** (dash line). The III-V and most II-VI semiconductors have direct gap energy.

Indirect Gap Semiconductors: Fig 4.2(b) shows the **E-k** diagram for indirect gap semiconductor along the [100] and [111] directions. It is seen that the valence band maximum and lowest conduction band minimum are saturated at different values of **k**. In such semiconductor, the direct transition of electron from the valence band to the conduction band by a photon of energy E_g is not possible. This happens because a photon has a very small momentum and an electron suffers a large change in momentum. However, a non vertical transition can occur indirectly by the cooperation of the lattice phonon which can supply the required momentum. The vertical transition are also possible for $h\nu > E_g$, where E_g is the direct gap energy.

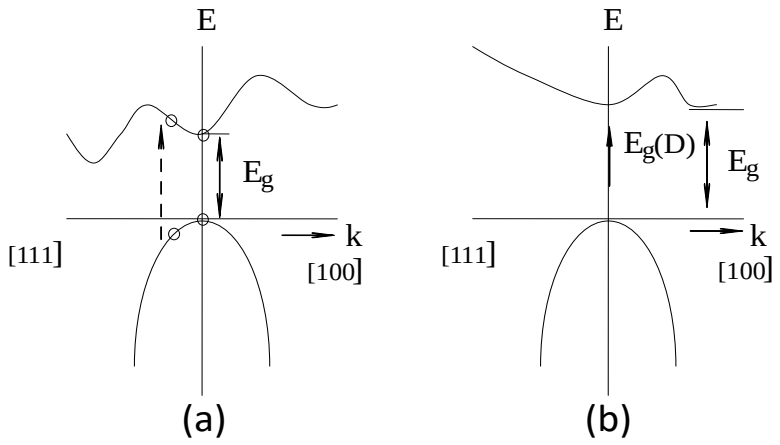

Fig 4.2 E-k plots for (a) Direct gap and (b) Indirect gap semiconductor

4.3 Transmittance (T)

In spectroscopy, transmittance is the fraction of incident light at a specified wavelength that passes through a sample. A related term is absorptance, which is the fraction of light absorbed by a sample at a specified wavelength. The ratio of transmitted energy to the amount of incident energy is called transmittance. Transmittance was formerly called transmission. Occasionally one also hears the terms visible transmittance (VT) and visible absorptance (VA), which are the respective fractions for the spectrum of visible light. The transmittance is simply the fraction of light in the original beam that passes through the sample and reaches the detector. The remainder of the light, 1 - *T*, is the fraction of the light absorbed by the sample. If no light is absorbed, the absorbance is zero (100% transmittance). Each unit in absorbance corresponds with an order of magnitude in the fraction of light transmitted. For $A = 1$, 10% of the light is transmitted ($T = 0.10$) and 90% is absorbed by the sample. For *A*

= 2, 1% of the light is transmitted and 99% is absorbed. For A = 3, 0.1% of the light is transmitted and 99.9% is absorbed. Transmittance values can be easily derived from the formulas given above.In equation form,

$$T = \frac{I}{I_0}$$

where I_0 is the intensity of the incident light and I is the intensity of the light coming out of the sample. In these equations, scattering and reflection are considered to be close to zero or otherwise accounted for. The transmittance of a sample is sometimes given as a percentage. Transmittance is related to absorbance A (not to be confused with absorptance) as

$$A = -\log_{10} T = -\log_{10}\left(\frac{I}{I_0}\right)$$

or, using the natural logarithm

$$A = -\ln T = -\ln\left(\frac{I}{I_0}\right)$$

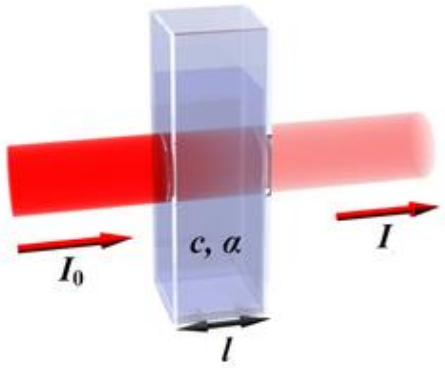

Fig 4.3 Diagram of Beer-Lambert Law of transmittance of a beam of light

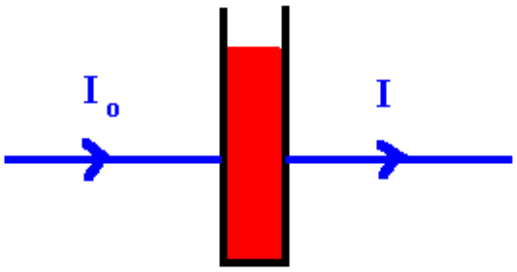

Fig 4.4 Transmittance and Absorbance

4.4 Absorbance (A)

Absorption is a process in which incident radiated energy is retained without reflection or transmission on passing through a medium. Absorbance values can be easily converted into transmittance, percent transmittance or reflectance values using the following equations:

In spectroscopy, the absorbance

$$A = -\log_{10} T = -\log_{10}\left(\frac{I}{I_0}\right),$$

where I is the intensity of light at a specified wavelength λ that has passed through a sample (transmitted light intensity) and I_0 is the intensity of the light before it enters the sample or incident light intensity. Absorbance measurements are often carried out in analytical chemistry, since the absorbance of a sample is proportional to the thickness of the sample and the concentration of the absorbing species in the sample, in contrast to the transmittance I / I_0 of a sample, which varies logarithmically with thickness and concentration. Absorbance spectra are typically used to define photopigment spectra because their shape, when normalized (i.e., plotted as a fraction of the maximum absorbance), is independent of pigment optical density (pigment concentration). In contrast, the absorbance spectra, like the spectral sensitivity of the human subject, broaden as the optical density increases. Absorbance is

the measure of the quantity of light that a sample neither transmits nor reflects and is proportional to the concentration of a substance**.** The transmittance of a sample is the ratio of the intensity of the light that has passed through the sample to the intensity of the light when it entered the sample ($T = I_{out} / I_{in}$). The transmittance is displayed as a percentage on the top scale of the meter. To convert between the absorbance and transmittance scales, use the equation:

Absorbance = -log (percent transmittance/100)

Absorbance does not have true units, it is quite often reported in "Absorbance Units" or AU (not to be confused with the Astronomical unit).

4.5 Absorption coefficient (α)

The absorption coefficient determines how far into a material light of a particular wavelength can penetrate before it is absorbed. In a material with a low absorption coefficient, light is only poorly absorbed, and if the material is thin enough, it will appear transparent to that wavelength. The absorption coefficient depends on the material and also on the wavelength of light which is being absorbed. Semiconductor materials have a sharp edge in their absorption coefficient, since light which has energy below the band gap does not have sufficient energy to raise an electron across the band gap. Consequently this light is not absorbed. The absorption coefficients α of the films have been calculated from the experimentally measured values of A and T according to the following relation. The optical absorption coefficient α is determined using the relation

$$\alpha = \left(\frac{2.303}{t}\right)\left[\log\left(\frac{1}{T}\right)\right]$$

where, t is the thickness of the sample. In SI units, absorption coefficient is measured in inverse meters, and is represented by the Greek letter. In chemistry and biological sciences, the absorption coefficient is a measure of the solubility

of a gas in a liquid measured as the volume of the gas (taken under standard conditions) that saturates a unit volume of the liquid.

4.6 Extinction Coefficient (k)

Extinction Coefficient is the fraction of light lost to scattering and absorption per unit distance in a participating medium. In electromagnetic terms extinction coefficient can be explained as the decay, or damping of the oscillation amplitude of the incident electric field. Extinction coefficient refers to several different measures of the absorption of light in a medium:

- In chemistry, the mass extinction coefficient (also called mass attenuation coefficient or mass absorption coefficient) and the molar extinction coefficient are parameters defining how strongly a substance absorbs light at a given wavelength, per mass unit or per molar concentration, respectively.
- In physics, the "extinction coefficient" is the imaginary part of the complex index of refraction, which also relates to light absorption.

which the absorption coefficient (α) can be expressed in terms of the extinction coefficient (*k*) as:

$$\alpha = \frac{4\pi fk}{c}$$

As the velocity of light in a vacuum, c = fλ, then α = 4πk/λ. This equation is known as Bouguer's law or Lambert's law of absorption, by which radiation is absorbed to an extent that depends on the wavelength of the radiation and the thickness and nature of the medium.

4.7 Band Gap Energy

The energy spectrum of an electron moving in a periodic potential consists of a set of allowed energy regions or bands which are separated by forbidden energy regions called the band gap. The band gap energy is the energy needed to break a bond in the crystal. When a bond is broken, the electron has absorbed enough energy to leave the valence band and "jump" to the conduction band. The width of the band gap determines the type of material (conductor, semiconductor, insulator) we are working with. This is shown pictorially using a band diagram.

The energy gap of the thin film was obtained by plotting α^2 vs wavelength. The straight–line part of the graph was extrapolated to meet the wavelength axis at λ at the point where $\alpha^2=0$. The wavelength obtained at this point depicts the wavelength of the radiation film. The band-gap was then obtained from the relation:

$$\alpha^2 = \text{photon energy} - \text{band gap.}$$

$$\alpha^2 = h\nu - Eg$$

$$\alpha^2 = \frac{hc}{\lambda} - E_g$$

$$0 = \frac{hc}{\lambda} - E_g$$

$$E_g = \frac{hc}{\lambda}$$

The work that a physical system is capable of doing in changing from its actual state to a specified reference state, the total including, in general, contributions of potential energy, kinetic energy, and rest energy. A range of some physical variable, as of radiation wavelength or frequency. A range of very closely

spaced electron energy levels in solids, the distribution and nature of which determine the electrical properties of a material.

The transmission or conveying of something through a medium or passage, esp of electric charge or heat through a conducting medium without perceptible motion of the medium itself. The capacity of an atom or group of atoms to combine in specific proportions with other atoms or groups of atoms. A valence electron is in the outer or next outer shell of an atom and can participate in forming chemical bonds with other atoms.

4.8 Optical Measurements of Thin Films

The optical transmittance and absorbance spectra for Ag_2S thin films were obtained in ultraviolet/ visible region using a Shimadzu UV-240 UV/VIS spectrophotometer with uncoated glass slide as the reference.

The reflectance has been found by using the relationship:

$$R + T + A = 1$$

The energy band gap of deposited sintered films was determined using the transmission spectra. Optical transmittance spectra and absorbance spectra as a function of wavelength of Ag_2S thin films with different thickness are plotted in Fig 4.5 and 4.6.

The theory of optical transmission gives the relationship between the absorption coefficient α and the photon energy $h\nu$,

$$\alpha = -\frac{1}{d}\ln\frac{1}{T}$$

where d is film thickness (μm). The optical absorption gives the relationship between the absorption coefficient α and the photon energy $h\nu$ as

$$\alpha = \frac{(h\nu - Eg)^{1/2}}{\mathrm{h}\nu}$$

Fig 4.7 shows variation in $(\alpha h\nu)^2$ with photon energy ($h\nu$) for Ag_2S films in different thickness.

For normal reflectance $R = (n - 1)^2/ (n + 1)^2$

The relationship between refractive index and reflectance for semiconductors and insulators when $k^2 << n^2$.

$$n = \frac{1 + \sqrt{R}}{1 - \sqrt{R}}$$

where R is the normal reflectance; using the above relation the refractive index n was determined. Refractive index (n) and extinction coefficient (k) versus photon energy ($h\nu$) for Ag_2S thin films are shown in Fig 4.8 and 4.9, respectively.

The extinction coefficient k as a function of wavelength λ and absorption coefficient α were given by,

$$k = \frac{\alpha\lambda}{4\pi}$$

The optical conductivity was determined using the

$$\sigma = \frac{\alpha nc}{4\pi}$$

where c is the velocity of light. The increased optical conductivity at high photonenergies is due to the high absorbance of Ag_2S thin film in that region. Fig 4.10 shows optical conductivity (σ) versus photon energy ($h\nu$) of Ag_2S films.

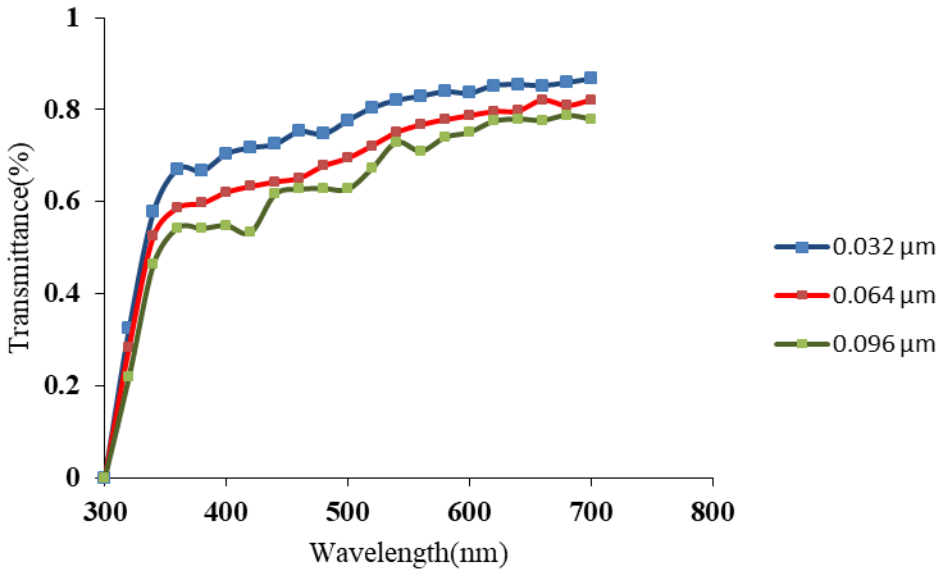

Fig 4.5 Optical transmittance spectra as a function of wavelength for thickness of Ag_2S film

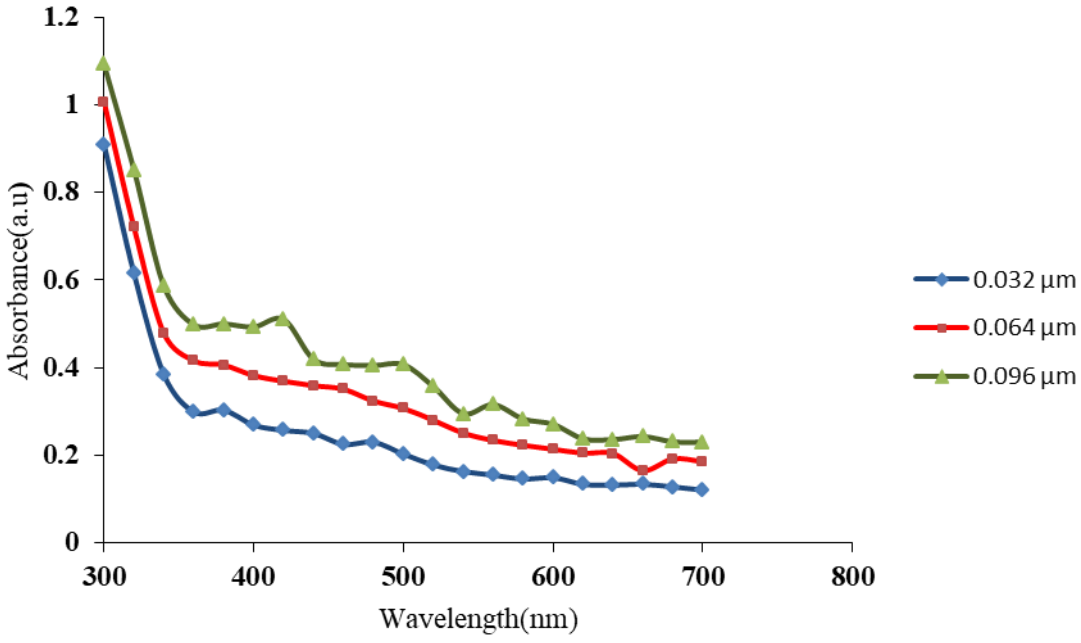

Fig 4.6 Plots of absorbance spectra of selected samples of Ag_2S thin films

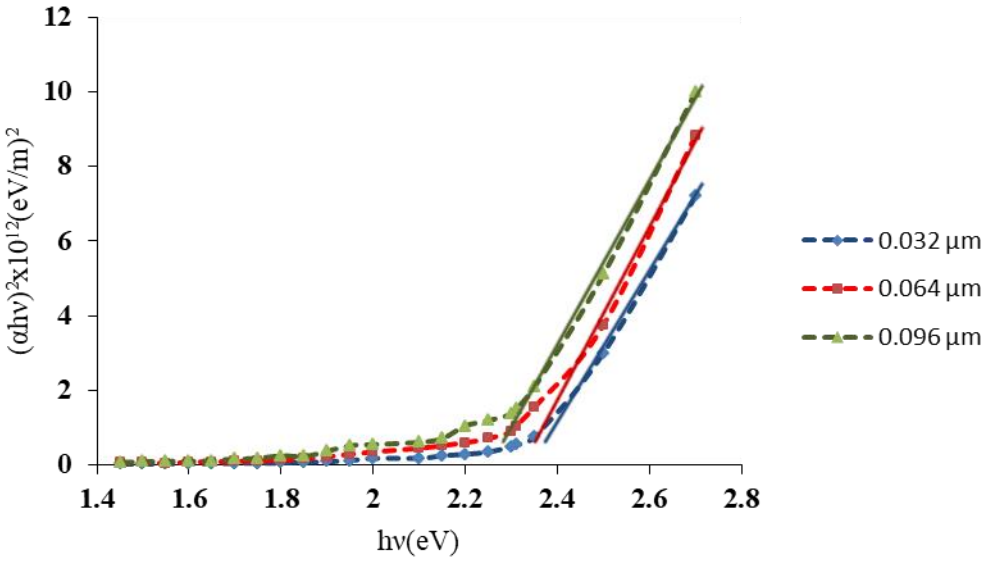

Fig 4.7 Variation in $(\alpha h\nu)^2$ with photon energy (hν) for Ag_2S films in different thickness

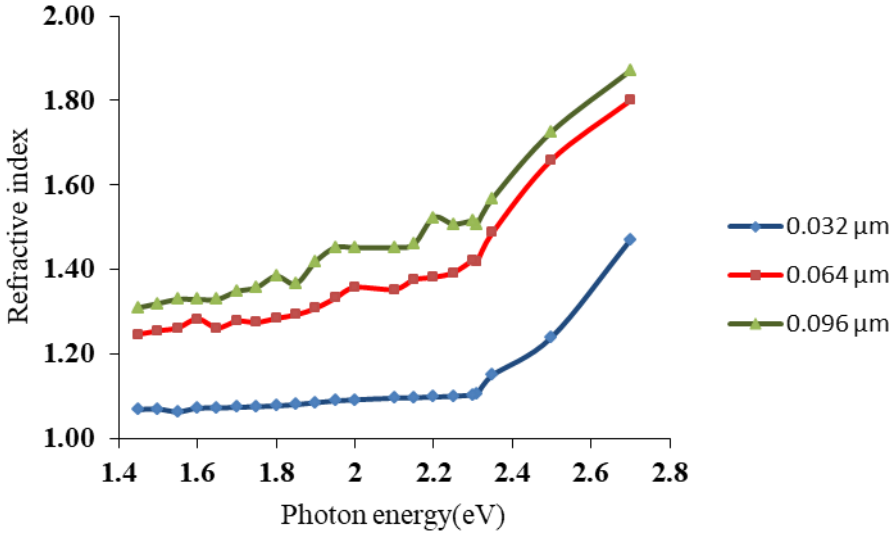

Fig 4.8 Refractive index (n) versus photon energy (hν) for Ag_2S thin films at different thickness

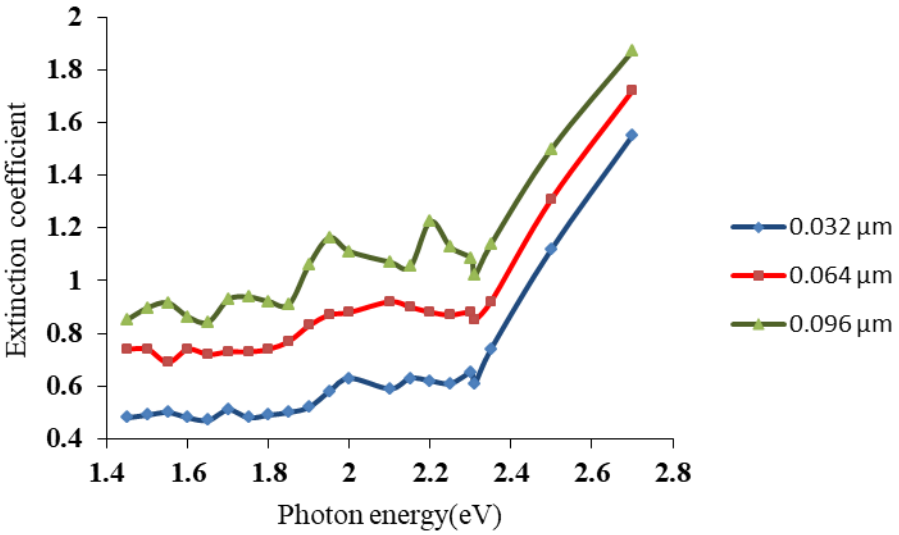

Fig 4.9 Extinction coefficient (k) versus photon energy (hν) for Ag_2S thin films with different thickness

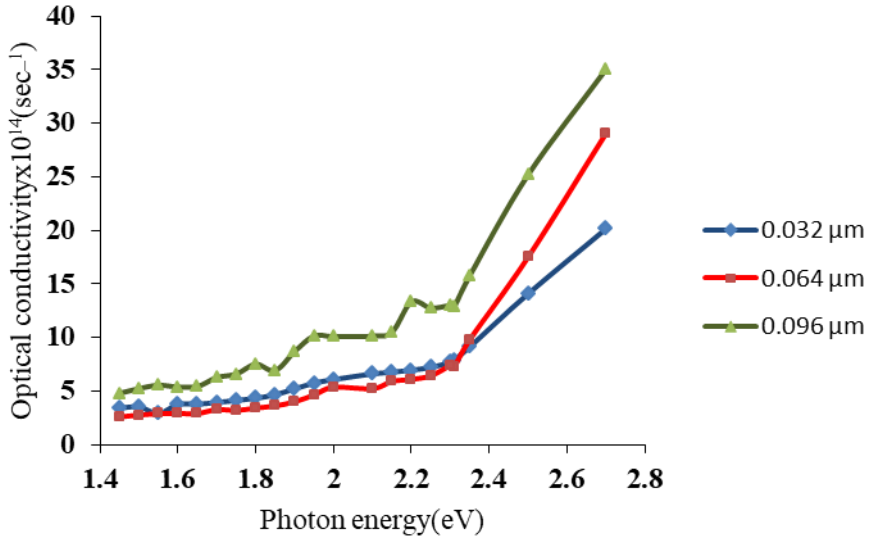

Fig 4.10 Optical conductivity (σ) versus photon energy(hν) of Ag_2S films

4.9 Photoconductivity Measurement

CHAPTER V

ELECTRICAL CHARACTERIZATION OF Ag_2S THIN FILMS

The surface resistivity of a material was determined using common techniques such as the four-point probe method and the Van der Pauw technique. The variations of the sheet resistance and light and dark electrical resistivity values of Ag_2S films in different deposition cycle were investigated at room temperature. The order of resistivity in the present work is in the range of 10^2-10^3 Ω cm. The Hall measurement, carried out in the presence of a magnetic field, yields the sheet carrier density n_s and the bulk carrier density n or p (for n- type or p- type material) if the conducting layer thickness of the sample is known.

5.1 Sample Preparation

Van der Pauw geometry was employed to measure resistivity of the Ag_2S film as shown in Fig 5.1. These measurements require that four corners ohmic contacts be placed on the square glass sample. Before the deposition, the glass substrates were washed in acetone and distilled water. Ag_2S thin films were prepared by CBD method onto the glass substrate. Four ohmic contacts were made of silver paste. They must be on the boundary of the sample. And then, this sample was fixed onto the spring clip board (four point probes). The spring clip sample mounting board makes sample mounting much quicker and easier. The average diameters (D) of the contacts, and sample thickness (d) must be much smaller than the distance between the contacts (L). Relative errors caused by non-zero values of D are of the order of D/L.

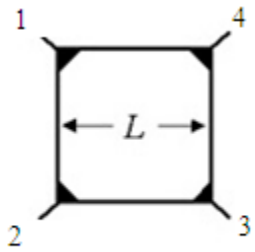

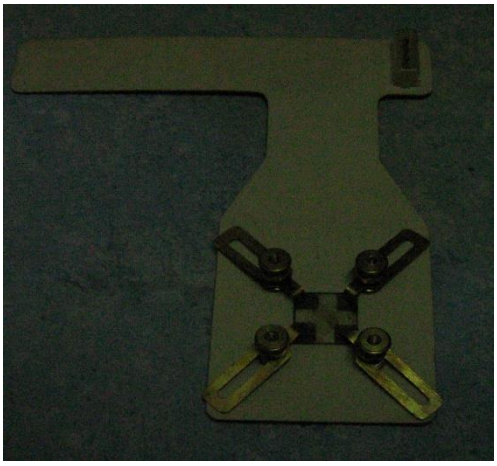

Fig 5.1 Sample geometry for Van der Pauw resistivity and Hall effect measurements

The following equipment is required:

• Permanent magnet, or an electromagnet (500 to 5000 gauss)

• Constant-current source with currents ranging from 10 μA to 100 mA (for semiinsulating GaAs, $\rho \sim 107\ \Omega\cdot$cm, a range as low as 1 nA is needed)

• High input impedance voltmeter covering 1 μV to 1 V

• Sample temperature-measuring probe (resolution of 0.1 °C for high accuracy work)

5.2 The Hall Effect and the Lorentz Force

The basic physical principle underlying the Hall effect is the Lorentz force. When an electron moves along a direction perpendicular to an applied magnetic field, it experiences a force acting normal to both directions and moves in response to this force and the force effected by the internal electric

field. For an n-type, bar-shaped semiconductor shown in Fig 5.2 , the carriers are predominately electrons of bulk density n. A constant current I was assumed that flows along the a-axis from left to right in the presence of a z-directed magnetic field. Electrons subject to the Lorentz force initially drift away from the current line toward the y-axis, resulting in an excess surface electrical charge on the sides of the sample. The force on holes is toward the same side because of their opposite velocity and positive charge. This transverse voltage is the Hall voltage V_H and its magnitude is equal to IB/qnd, where I is the current, B is the magnetic field, d is the sample thickness, and q(1.602×10^{-19}C) is the elementary charge. In some cases, it is convenient to use layer or sheet density (n_s =nd) instead of bulk density.

$$n_s = IB/q|V_H|$$

By measuring the Hall voltage V_H and from the values of I, B and q, the sheet density n_s of charge carriers in semiconductors can be determined. The Hall voltage is negative for n-type semiconductors and positive for p-type semiconductors. The sheet resistance R_s of the semiconductor can be conveniently determined by use of the van der Pauw resistivity measurement technique. Sheet resistance involves both sheet density and mobility, the Hall mobility can be determined from the equation

$$\mu = |V_H|/R_s IB = 1/(qn_s R_s)$$

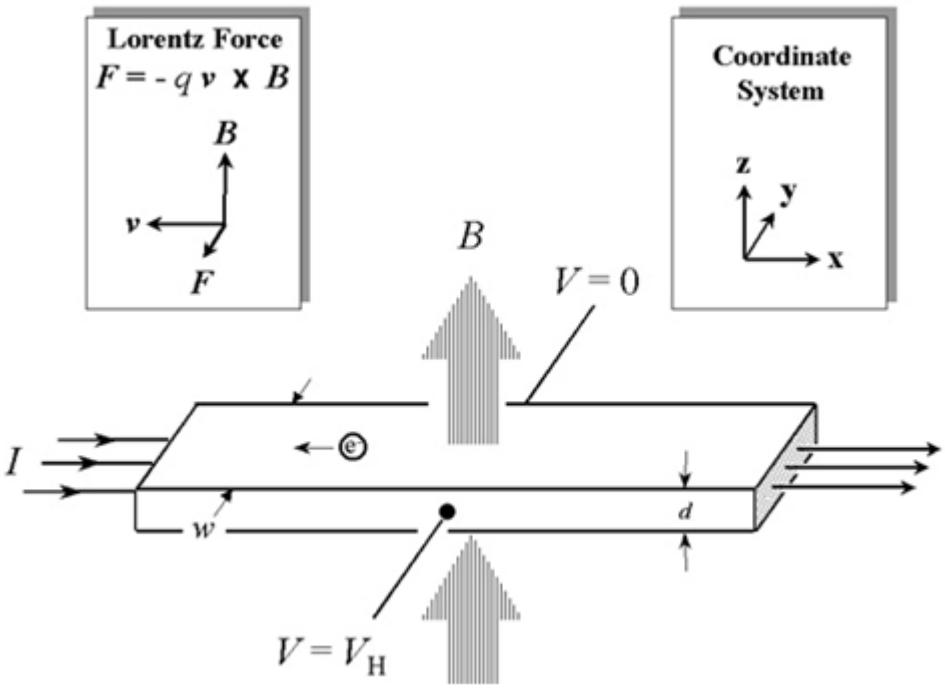

Fig 5.2 Schematic of the Hall effect in thin films with four ohmic contacts

5.3 Van der Pauw Technique

The Van der Pauw technique, due to its convenience, is widely used in the semiconductor industry to determine the resistivity of uniform samples. As originally devised by Van der Pauw, one uses an arbitrarily shape, thin-plate sample containing four very small ohmic contacts placed on the periphery, preferably in the corners, of the plate. A schematic of a rectangular Van der Pauw configuration is shown in Fig 5.3.

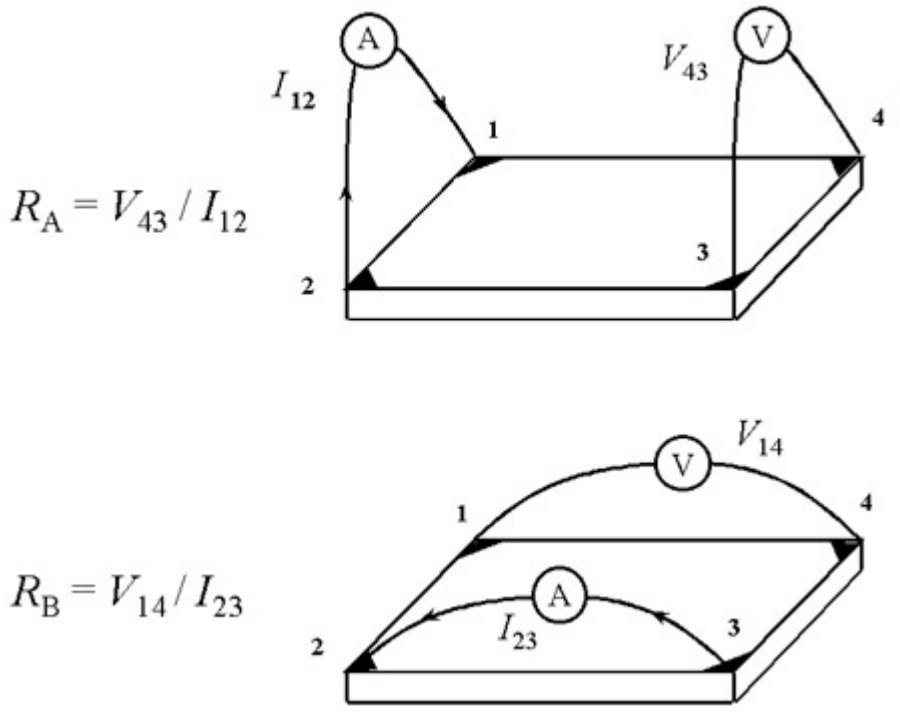

Fig 5.3 Schematic of a Van der Pauw configuration used in the determination of the two characteristic resistances R_A and R_B

The objective of the resistivity measurement is to determine the sheet resistance R_S. Van der Pauw demonstrated that there are actually two characteristic resistances R_A and R_B, associated with the corresponding terminals shown in Fig 5.3. R_A and R_B are related to the sheet resistance R_S through the Van der Pauw equation:

$$exp(-\pi R_A/R_S) + exp(-\pi R_B/R_S) = 1$$

which can be solved numerically for R_S. The bulk electrical resistivity ρ can be calculated using:

$$\rho = R_S d$$

To obtain the two characteristic resistances, one applies a dc current I into contact 1 and out of contact 2 and measures the voltage V_{43} from contact 4 to contact 3 as shown in Fig 5.3. Next, one applies the current I into contact 2 and out of contact 3 while measuring the voltage V_{14} from contact 1 to contact 4. R_A and R_B are calculated by means of the following expressions:

$$R_A = V_{43}/I_{12} \text{ and } R_B = V_{14}/I_{23}$$

The objective of the Hall measurement in the Van der Pauw technique is to determine the sheet carrier density n_s by measuring the Hall voltage V_H. The Hall voltage measurement consists of a series of voltage measurements with a constant current I and a constant magnetic field B applied perpendicular to the plane of the sample. Conveniently, the same sample, shown again in Fig 5.4, can also be used for the Hall measurement.

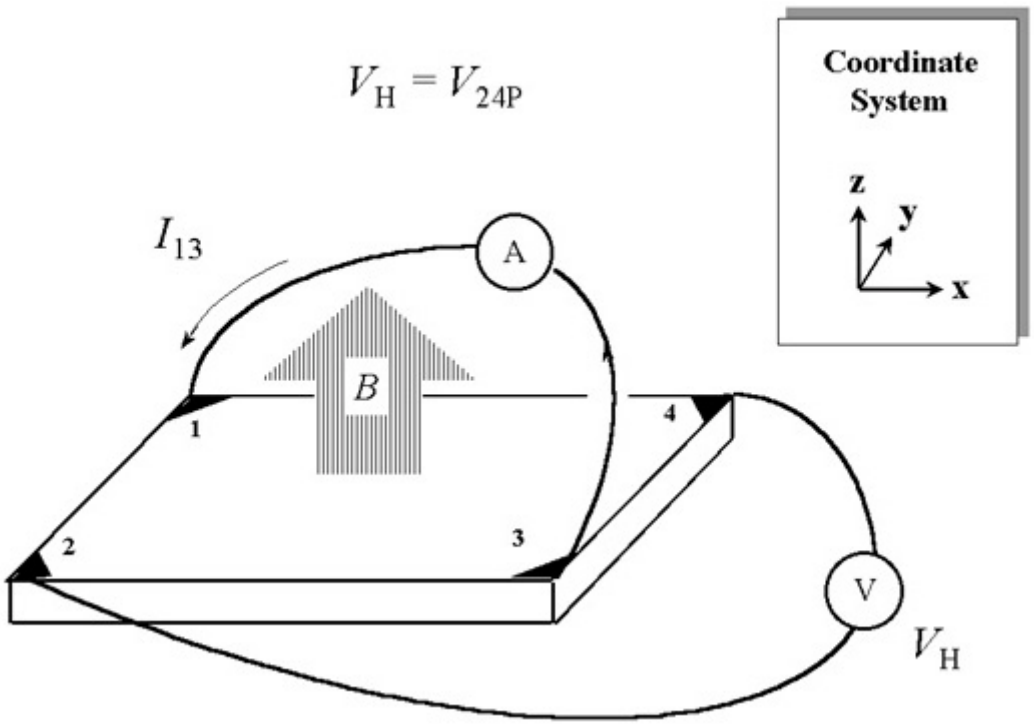

Fig 5.4 Schematic of a Van der Pauw configuration used in the determination of the Hall voltage V_H.

To measure the Hall voltage V_H, a current I is forced through the opposing pair of contacts 1 and 3 and the Hall voltage V_H (= V_{24}) is measured across the remaining pair of contacts 2 and 4. Once the Hall voltage V_H is acquired, the sheet carrier density ns can be calculated via $n_s = IB/q|V_{H|}$ from the known values of I, B, and q. There are practical aspects which must be considered when carrying out Hall and resistivity measurements. Primary concerns are (1) ohmic contact quality and size, (2) sample uniformity and accurate thickness determination, (3) thermomagnetic effects due to nonuniform temperature, and (4) photoconductive and photovoltaic effects which can be minimized by measuring in a dark environment. Also, the sample lateral dimensions must be large compared to the size of the contacts and the sample thickness. Finally, one must accurately measure sample temperature, magnetic field intensity, electrical current, and voltage.

5.4 Resistivity Measurements and Calculations

The data must be checked for internal consistency, for ohmic contact quality, and for sample uniformity. A dc current I was set up and the current I_{21} was applied and voltage V_{34} was measured. Next, the polarity of the current (I_{12}) was reversed and measure V_{43} was measured. The remaining six values (V_{41}, V_{14}, V_{12}, V_{21}, V_{23}, V_{32}) were repeated. Eight measurements of voltage yield the following eight values of resistance, all of which must be positive:

$R_{21,34} = V_{34}/I_{21}$, $R_{12,43} = V_{43}/I_{12}$,

$R_{32,41} = V_{41}/I_{32}$, $R_{23,14} = V_{14}/I_{23}$

$R_{43,12} = V_{12}/I_{43}$, $R_{34,21} = V_{21}/I_{34}$

$R_{14,23} = V_{23}/I_{14}$, $R_{41,32} = V_{32}/I_{41}$

It is noted that with this switching arrangement the voltmeter is reading only positive voltages, so the meter must be carefully zeroed.

Because the second half of this sequence of measurements is redundant, it permits important consistency checks on measurement repeatability, ohmic contact quality, and sample uniformity.

Measurement consistency following current reversal requires that:

$R_{21,34} = R_{12,43}$ $\qquad$ $R_{43,12} = R_{34,21}$

$R_{32,41} = R_{23,14}$ $\qquad$ $R_{14,23} = R_{41,32}$

The reciprocity theorem requires that:

$R_{21,34} + R_{12,43} = R_{43,12} + R_{34,21}$ and

$R_{32,41} + R_{23,14} = R_{14,23} + R_{41,32}$

The sheet resistance R_S can be determined from the two characteristic resistances

$R_A = (R_{21,34} + R_{12,43} + R_{43,12} + R_{34,21})/4$ and

$R_B = (R_{32,41} + R_{23,14} + R_{14,23} + R_{41,32})/4$

via the Van der Pauw equation . If the conducting layer thickness d is known, the bulk resistivity $\rho = R_S\, d$ can be calculated from R_S.

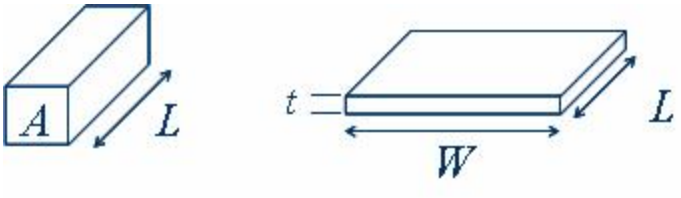

Fig 5.5 Geometry for defining resistivity (left) and sheet resistance (right)

5.5 Electrical Resistivity of Ag_2S Films

The resistivity of the films prepared by chemical methods is generally high as compared to single crystals. Room temperature electrical resistivity of Ag_2S films from a thiourea bath is of the order of 10^5 Ωcm, whereas from a thioacetamide bath it is of the order of 10^4 Ωcm[4]. Room temperature electrical resistivity of Ag_2S films was studied by the four- point probe method using silver contacts. It was observed that the resistivity from thiosulphate bath films is of the order of 10^2-10^3 Ωcm. The variation of electrical resistivity of Ag_2S films with film thickness is shown in Fig 5.6.

5.6 Hall Voltage Measurement of Ag_2S Films

Hall-effect measurements were performed at room temperature for films deposited on glass substrate to determine Hall voltage (V_H) and magnetoresistance. These measurements have been carried out using four ohmic contacts on the sample. Magnetoresistance were investigated by using Fluke 1520 Meg-ohmmeter. The graph of the magnetic field and magnetoresistance is shown in Fig 5.7. In this work, the order of magnetoresistance in the present film is in the ** MΩ - ** MΩ. Fig 5.8 illustrates the variation of Hall Voltage with current of Ag_2S thin film under the magnetic field of 500 mT. The range film exhibited the Hall voltage range of **mV – **mV at current driven to sample of **μA–** μA. The graph of current and Hall voltage is shown in Fig 5.9. V_H is directly proportional to B and V_H is directly proportional to I verifying the linear relation implied by equation $R_H = V_H t/IB$ (or) $V_H = R_H IB/t$. The Hall voltage of the present film was found varying with magnetic field.

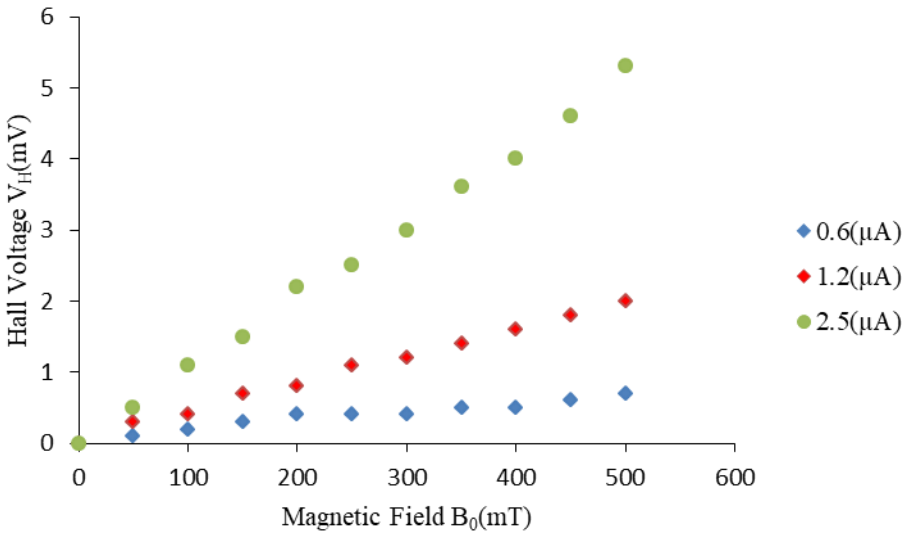

Fig 5.8 Variation of Hall voltages with Magnetic field

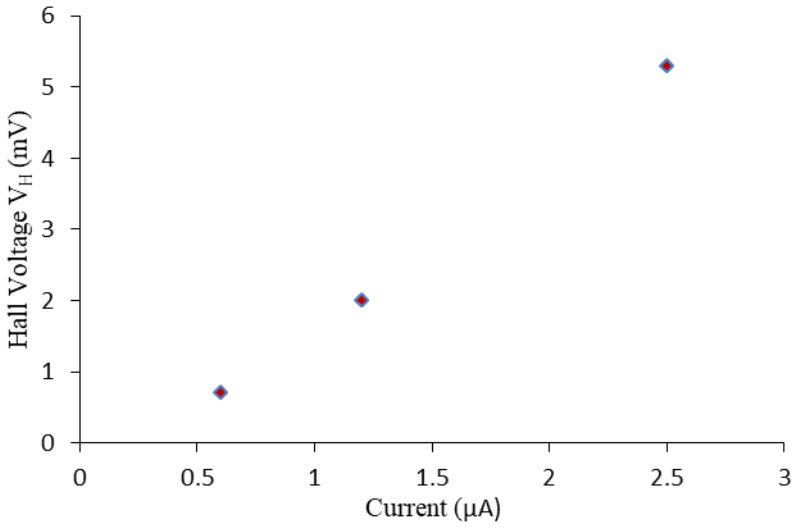

Fig 5.9 Variation of Hall voltages with current under the magnetic field of 500 mT

CHAPTER VI

RESULTS AND DISCUSSION

A simple and economical electroless chemical deposition technique for deposition of metal sulphide is presented. Aqueous solution of metal salts and of sodium thiosulphate was used for the chemical bath. The technique is based on hydrolytic decomposition of the metal- thiosulphate complex in aqueous media, at a suitable temperature, concentration and pH. The technique presented in this work has been successfully used for deposition of Ag_2S in alkaline media, on various substrates, such as glass, metal (Ni). Phase identification, microstructure properties, optical studies and electrical characterization of the deposited films were investigated. The Hall Effect measurement is essential to determine accurately the electrical properties of thin film.

6.1 Evolution of Crystalline Structure

X- ray studies of the films showed that the as-prepared films of Ag_2S were a mixture of both amorphous and polycrystalline phases, while Ag_2S/ Ni films were found to be polycrystalline. Annealing of the films of Ag_2S and Ag_2S/ Ni at 200 ºC for 3 h led to further crystallization. The X- ray diffraction patterns of as prepared and annealed Ag_2S and Ag_2S/ Ni films are shown in Fig 6.1 and 6.2, respectively.

The variation of lattice parameters, crystal system, average crystallite sizes and grain size of Ag_2S and Ag_2S/ Ni films are presented in Table 6.1. The crystalline structure evidenced for the as- deposited and annealed films matches well that of the monoclinic acanthite phase of Ag_2S.

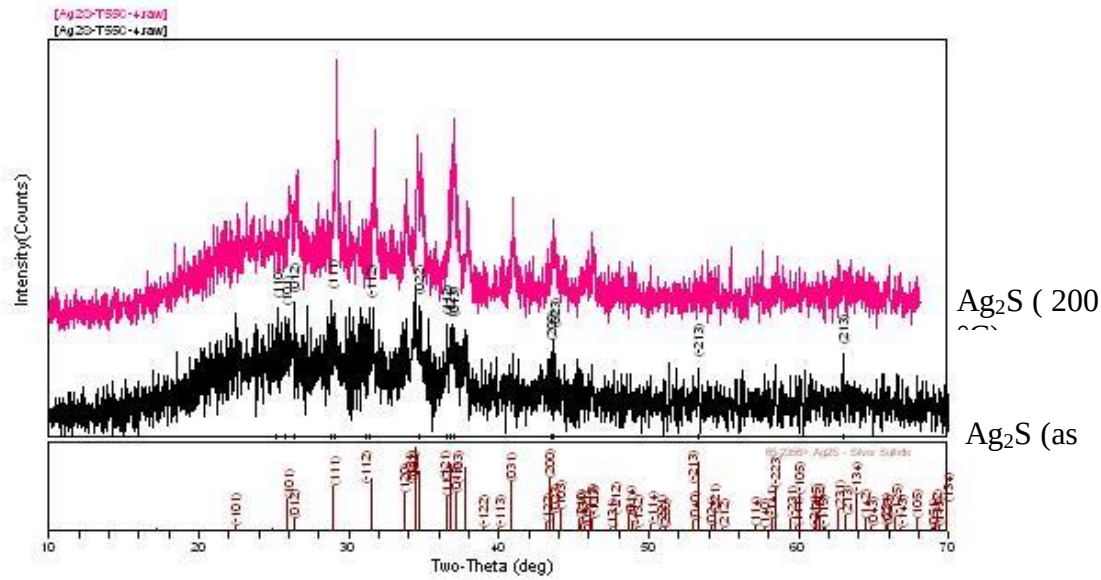

Fig 6.1 XRD patterns recorded for as prepared Ag_2S thin films on glass substrate and after heating in air at 200 ºC for 3h

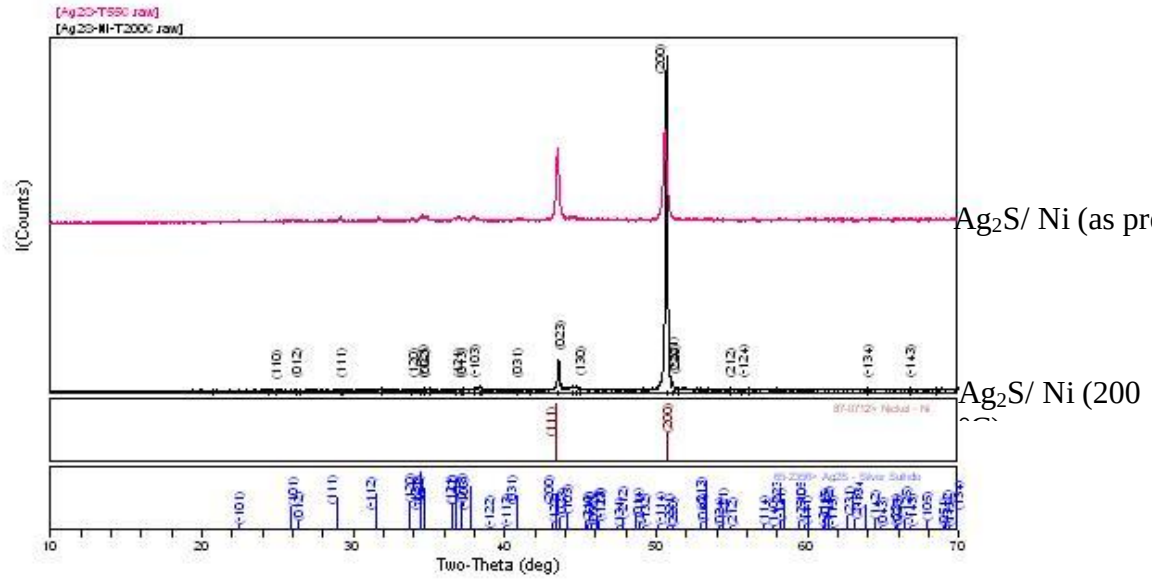

Fig 6.2 XRD patterns for an Ag_2S films deposited on Ni substrate and heated in air at 200ºC for 3h

Table 6.1 Variation of structural parameters, crystal system and average crystallite sizes and grain size of Ag_2S and Ag_2S/ Ni thin films

	Ag_2S		Ag_2S/ Ni	
	As prep.	Annealed	As prep.	Annealed
Lattice Constants (Å)	a = 4.2467 b= 6.8424 c= 7.8951 β= 99.34º	a= 4.2102 b=7.0227 c=7.7676 β=99.53 º	a = 4.2166 b= 6.8364 c= 7.9044 β= 99.73º	a= 4.2309 b=6.9156 c=7.9418 β=99.17 º
System	Monoclinic	Monoclinic	Monoclinic	Monoclinic
Average Crystallite Size from XRD (nm)	43.28	82.41	49.32	73.82
Average Grain Size from SEM (μm)	0.83	0.57	0.64	0.64

6.2 Microstructure of Ag_2S Thin Films

SEM micrographs of as deposited and annealed Ag_2S and Ag_2S/ Ni films are shown in Fig 6.3. The films contained a random distribution of small crystallites and at annealing temperature 200°C show the over-growth of particles on the smooth film surface. The films are thick, rough and dark grey in appearance. The grain size was estimated from the micrographs. The values of average grain size of as-deposited film and annealed Ag_2S and Ag_2S/ Ni thin films are presented in Table 6.1.

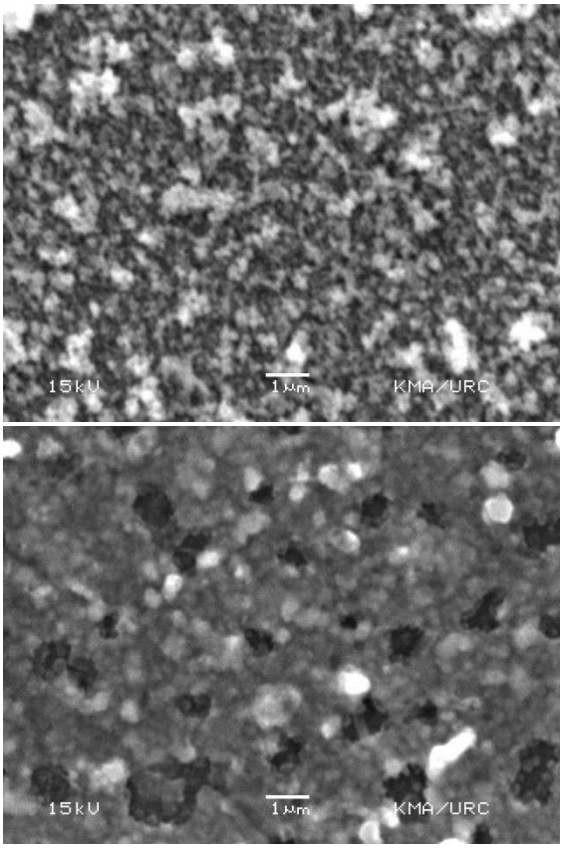

(a) (b)

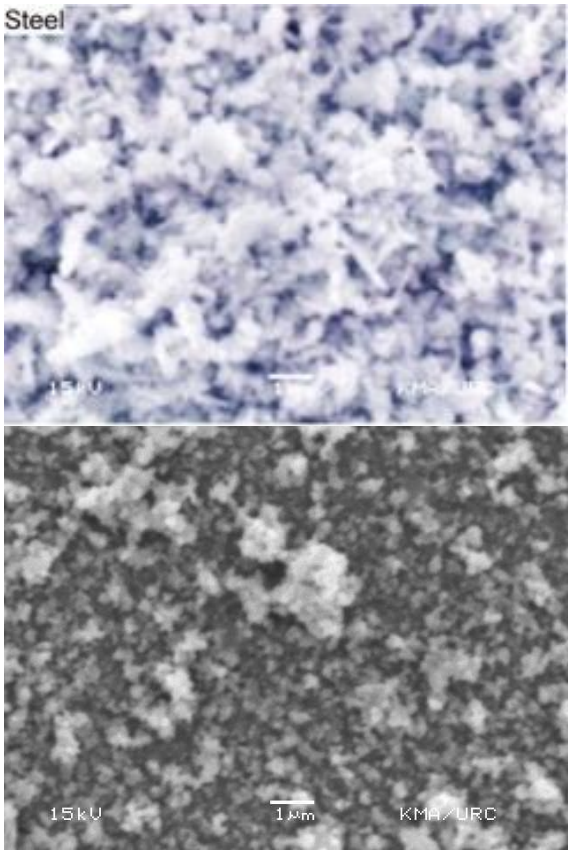

(c) (d)

Fig 6.3 Microstructure recorded using SEM of Ag_2S deposited on: the glass substrate, (a) as prepared, (b) after annealing at 200ºC; the nickel substrate, (c) as prepared and (d) after annealing at 200°C

Table 6.2 Variation of film thickness and deposition cycle for Ag_2S thin films

Sample	Deposition cycles	Thickness (µm)
Ag_2S-1	1	0.032
Ag_2S- 2	2	0.064
Ag_2S-3	3	0.096

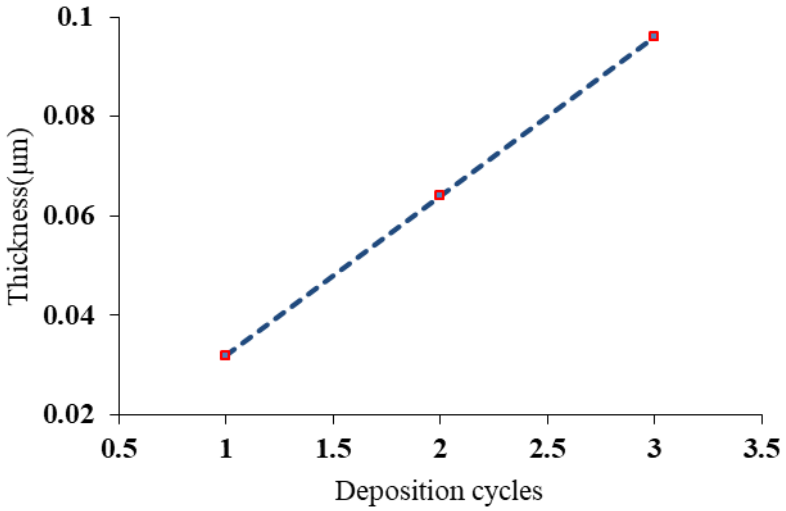

Fig 6.4 Plot of film thickness vs. deposition cycles for Ag_2S films

6.3 Optical Studies

The optical properties of Ag_2S thin films deposited on glass substrate for different thickness were determined from the absorbance (A) and transmittance (T) measurements in the range 300- 700 nm. Based on the obtained optical absorption measurements, the square of absorption coefficient $(\alpha h\nu)^2$ is plotted as a function of photon energy ($h\nu$). The variation of refractive index (n), extinction coefficient (k), optical conductivity (σ) and band gap energy (E_g) was given in Table 6.3. The high value of n, k and σ for the Ag_2S thin films was found to be at energy ($h\nu$) equal to 2.7 eV. The optical film's two parameters have been correlated with each other; when the refractive index decreases, the value of the optical band gap increases.

Table 6.3 Variation of refractive index (n), extinction coefficient (k), optical conductivity (σ) and band gap energy ($h\nu$) of Ag_2S films

Sample	Refractive index	Extinction coefficient	Optical conductivity (sec^{-1})	Band gap energy (eV)
Ag_2S-1	1.52	1.55	20.08×10^{14}	2.33
Ag_2S- 2	1.79	1.72	29.01×10^{14}	2.32
Ag_2S-3	1.92	1.87	36.02×10^{14}	2.25

6.4 Electrical Characterization of Ag_2S Thin Films

The sheet resistance (R_s) and the bulk electrical resistivity (ρ) were determined at room temperature in dark, room light and sunlight conditions by using four-point probe. All films exhibit semiconducting behaviors with resistivity in the range of 10^2- 10^3 Ω cm, increasing with film thickness. These remarkable results are given in Table 6.4. The resistivity increased with increasing the film thickness. It can be seen that the thickness (*d*) of Ag_2S films has been found to have important effect on the light and dark electrical resistivity. So, it was determined that all the films are photosensitive materials.

Table 6.4 Basic electrical characteristics of Ag_2S films without applying magnetic field

Thickness d (μm)	Sheet resistance R_s × 10^6 (Ω/ square)			Resistivity ρ × 10^3 (Ωcm)			Conductivity σ × 10^{-3} $(\Omega cm)^{-1}$		
	Dark	Light	Sunlight	Dark	Light	Sunlight	Dark	Light	Sunlight
0.032	18.41	19.7	26.90	0.058	0.062	0.089	17.24	16.12	11.23
0.064	13.66	14.70	17.60	0.087	0.094	0.112	11.49	10.63	8.92
0.096	12.80	12.40	9.30	0.122	0.119	0.089	8.19	8.40	11.23

6.5 Conclusions

The chemical bath deposition methods are simple, inexpensive and convenient for large area deposition and capable of yielding nanocrystalline thin films. The XRD patterns of as- prepared and annealed Ag_2S and Ag_2S/ Ni films have been presented. The film materials deposited from alkaline baths were predominantly polycrystalline. Further crystallization was easily achieved by 3 h annealing and at 200ºC. The films showed optical band gap between 2.25 eV-2.33 eV with electrical resistivity of ~10^3 Ωcm. The films show n- type electrical conductivity. The high optical absorption coefficient in the visible region, suggested it as an effective absorber material for solar energy.

REFERENCES

[1] Acharya H N and Bose H N 1971 *Phys. Stat. Sol. A,* ***6*** K43.

[2] Chopra K L, Kainthla R C, Pandya D K and Thakeoor A P 1982 *Phys. Thin Films****, 102*** 167.

[3] Dhumure S S and Lokhande C D 1991 *Mater. Chem. Phys.*, ***27*** 321.

[4] Dhumure S S and Lokhande C D 1992 *Solar Energy Mater. Solar Cells,* ***28*** 159.

[5] Hodes G 2002 Chemical Solution Deposition of Semiconductor Films. Marcel Dekker, Inc, New York

[6] Mangalam M J, Rao K N, Rangarajan N and Suryanarayana C V 1969 *Ind. J. Pure Appl. Phys.*, ***7*** 628.

[7] Pavaskar N R, Manezes C A and Sinha A P B 1977 *J. Electrochem. Soc.,* ***124*** 743.

[8] Rai B K, Bist H D, Katiyar R S,Nair M T S, Nair P K and Mannivannan A1997 *J. Appl. Phys.* ***82*** *13 10*